Behavioral Model of Hydrogen Bonding Network for Digital Signal Processing

ELITSA EMILOVA GIEVA, ROSTISLAV PAVLOV RUSEV, GEORGE VASILEV ANGELOV, ROSSEN IVANOV RADONOV, TIHOMIR BORISOV TAKOV and MARIN HRISTOV HRISTOV
Department of Microelectronics
Technical University of Sofia
Sofia 1000, Kliment Ohridski bul.8
BULGARIA
gieva@ecad.tu-sofia.bg, rusev@ecad.tu-sofia.bg, gva@ecad.tu-sofia.bg, radonov@ecad.tu-sofia.bg, takov@ecad.tu-sofia.bg, mhristov@ecad.tu-sofia.bg http://ecad.tu-sofia.bg

Abstract: A circuit schematic is extracted from *β*-lactamase protein hydrogen bonding network. The circuit is consisting of block-elements that functionally represent the hydrogen bonds. The behavioral description of each block element is represented by polynomials. Polynomials and electric connections between the elements are coded in Matlab and Verilog-A. DC, transient, and digital analyses are performed. Simulations proved that the circuit can process digital signals and behaves similarly to current mirror, amplifier, and inverter.

Key-Words: Hydrogen bonding network, behavioral modeling, Verilog-a, proteins, β-lactamase;

1 Introduction

Molecular electronics is often suggested as a potential successor to the conventional Si-based CMOS electronics, due to its advantages related to size, cheapness of fabrication, chemical tunability and 'bottom-up' self-assembly. However, progress has been withhold by difficulties such as formation of stable junctions and reproducibility of molecular currents measurements. The situation has improved considerably over the last few years. The greatest advantage of organic molecules versus inorganic materials for electronic applications is their capacity to self-assemble into complex and, at times, functional architectures.

Molecular electronics is based on the development of organic and biological materials within electronic and optoelectronic devices. Conventional electronics shifted to molecular electronics by implementing molecular materials in electronic and optoelectronic devices utilizing the unique features of organic compounds macroscopic. The most widely known commercial product so far are the liquid crystal displays (LCDs). However, after many years of research, the organic light-emitting devices (LEDs) based on dyes and polymers, synthetic electronic circuits, chemical and biochemical sensors have drawn attention [1].

Bioelectronics is associated with the direct coupling of biomolecular function units of high molecular weight and complicated molecular structure with electronic or optical transducer devices. Alternative and new concepts are developed for future signal processing technologies to address, control, read and write information. This requires the development of structures for signal transduction, amplification, processing and conversion [2].

Large part of bioelectronics research is focused on biopolymers such as photoactive yellow protein (PYP) [3] end green fluorescent protein (GFP) [4]. For development of different sensor, the transmembrane proton transfer protein – bacteriorhodopsin [5] long ago is used. It operates as a proton pump that is actuated by light. Commonly accepted opinion is to use bacteriorhodopsin as a molecular electronic material for construction of memories [6], i.e. for digital data storage.

Hydrogen bonds play a key role in biopolymers. Interesting analogies between hydrogen bonds and microelectronic logic gates can be derived. For example enol hydrogen bond serves as basis for AND, OR, NAND, NOR logic gates [7].

In our research so far, we have simulated the analog behavior of protein hydrogen bonding (HBN) networks and we have proved that they can operate as amplifiers, signals sources, modulators, shifters, etc. [8, 9]. The diverse nature of HBN behavior with analog signals observed in our previous papers induced us to study their digital properties.

In this paper we will investigate the digital behavior of an electrical circuit that is analogous to *β*-lactamase protein hydrogen bonding network.

2 Circuit and Equations

After extraction of hydrogen bonding network from β-lactamase protein we investigate the proton transfer characteristics of each of each hydrogen bond using protein electrostatic theory and Markus theory [10].

The main equation derived from Markus theory is given in Eq. (1). Here K [J/mol] is the proton transfer parameter that is proportional to proton current.

$$K = \frac{k_B T}{2\pi} \exp(-\frac{Eb - h\omega/2}{k_B T}) \quad (1)$$

where K – proton transfer parameter, k_B – Boltzmann constant, Eb – energy of the barrier, h – Plank constant, ω – frequency, T – temperature (in Kelvin). The barrier energy is calculated by:

$$Eb = (s_A(R(DA) - t_A)^2 + v_A) + s_B E_{12} + (s_C \exp(-t_C(R(DA) - 2)) + v_C)(E_{12})^2 \quad (2)$$

where $R(DA)$ is the distance between donor and acceptor, $E12$ is the difference between the energies of donor and acceptor.

After calculation of proton transfer characteristics of each hydrogen bond in the HBN we create the respective microelectronic block-elements to emulate the HBN operation. The HBN is divided in heavy atoms that form the hydrogen bonds (Fig. 1).

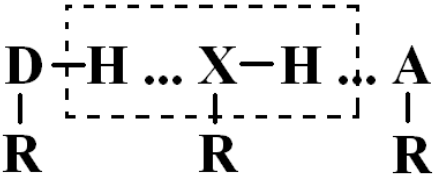

Fig. 1 Sample HBN with its heavy atoms X, D, and A.

In the analogous circuit each heavy atom (which is both donor and acceptor, designated with 'X') is represented as a separate block-element (Fig. 2).

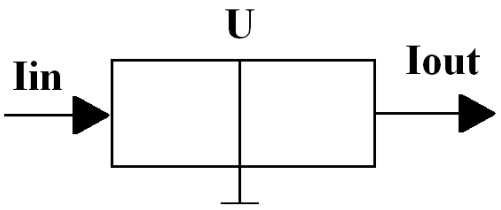

Fig. 2 Block-element that is analogous to heavy atom from the hydrogen bonding network.

In Fig. 2 the acceptor part of the heavy atom 'X' is assigned as the input of the respective block-element where the input current I_{in} flows in; the donor part of the heavy atom 'X' is assigned as the output of the respective block-element, where the output current I_{out} flows out. The potentials at the input and the output of the block-element are equal to the potential U of the heavy atom. The magnitude of the input and output currents are proportional to the proton transfer parameter of the hydrogen bonding network where the heavy atom is present.

The block-elements representation reduces the number of parameters originally present in Markus theory equations. We construct three- and four-terminal elements in the way shown above to prepare the HBNs for microelectronics treatment: the block-elements approach allows for simulation of the proton transport in hydrogen bonding networks. The relation between the input and output currents can be expressed by the parameter U – the potential of the heavy atom. Similarly, the two- and three terminal block-elements can be treated where the currents also can be expressed by the same parameter U. Block-elements also allows for modeling electronic circuits that are functionally analogous to the respective hydrogen bonding networks.

Using the block-elements approach we can describe the circuit behavior in Verilog-A [11] hardware description language and simulate it in Cadence Spectre simulator [12].

The HBN is taken from [9] and is shown in Figure 3. The HBN only consists of β-lactamase protein residues without water molecules (this is important fact because most of the protein HBNs include water molecules surrounding the protein).

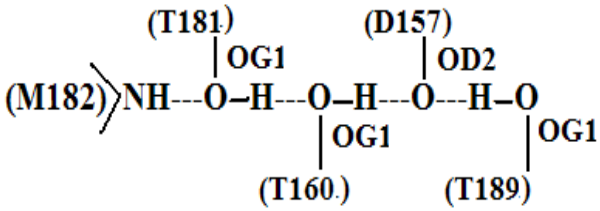

Fig. 3. Hydrogen bonding network (M1) without water molecules. (M182) is methionine residue, OG1 is hydroxyl oxygen of threonine residues (T160,181,189), OD2 is carboxyl oxygen of aspartic acid residue (D157).

In the HBN in Fig. 3 the M182N is a strong proton donor and it can act as microelectronic current source. The D157OD2 is a strong proton acceptor and it can be expressed as circuit output that sums two different signals. The rest of the circuit elements are described as three-terminal block elements. Each of them has equal input and output voltages and different current.

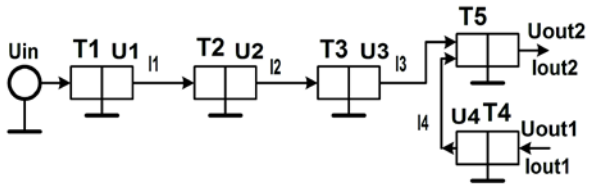

Fig. 4. Electrical circuit functionally analogous to hydrogen bonding network (M1).

The circuit functionally analogous to the hydrogen bonding network is given in Fig. 4. The three-terminal block elements are studied in [8]. The *I-V* characteristics of the block elements are analogous to the *K-V* characteristics of the hydrogen bonding networks studied in [9]. The current (*I*) in each block element corresponds to the proton transfer parameter (*K*) of each hydrogen bond and the voltage (*V*) of each block element corresponds to the electrostatic potential (El.pot.) [8]. The block elements are described by polynomials of different orders. The respective equations are coded in Matlab [14].

The circuit in Fig. 5 is implemented in Cadence [12]. It is identical to the circuit in Fig. 4. The block-elements are described in Verilog A hardware description language [11]. The current and voltage relations are expressed by polynomials of different orders. Some of the block-element equations in Verilog A are given below. The rest of the equations are similar.

The equations for block element T1 that is analogous to M182N is given below

$$U_1 = U_{in} \{-2.1 \text{ to } 2.65\} \quad (3)$$

$$I_1 = 8.10^{-5}\times U_1^4 - 7.10^{-5}\times U_1^3 - 0.001\times U_1^2 + 0.0048\times U_1 + 0.2516; \quad (4)$$

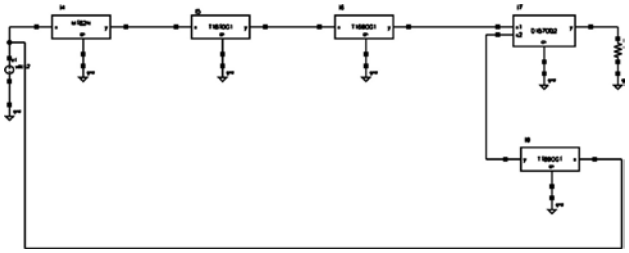

Fig. 5. Circuit of HBN M1 in Cadence.

The following equations are for T2 block element that corresponds to T181OG1:

$$U_2 = 0.9765\times U_1 + 0.074; \quad (5)$$

$$I_2 = -0.00011\times U_2^3 + 0.00032\times U_2^2 + 0.0012\times U_2 + 0.0081; \quad (6)$$

The equations below describe the current and voltage of T3 that is functionally analogous to T160OG1.

$$U_3 = 1.0321\times U_2 + 0.0519; \quad (7)$$

$$I_3 = 0.00013U_3^3 - 0.0003\, U_3^2 - 0.0018U_3 + 0.0104; \quad (8)$$

In a similar way are expressed the equations of T4 block element that corresponds to T189OG1 and is the first input of the circuit (U1out, I1out)

$$U_4 = 0.0031\times U_1^3 - 0.0616\times U_1^2 + 1.06\times U_1 + 0.5256; \quad (9)$$

$$I_4 = +0.76\times 10^{-5}\times U_4^3 - 2.1\times 10^{-5}\times U_4^2 - 0.0001\times U_4 + 0.00066; \quad (10)$$

The next circuit output is the T5 block element describing D157OD2. Its equations are:

$$U_5 = 0.9608\times U_4 - 0.0034; \quad (11)$$

$$I_5 = I_3 + I_4; \quad (12)$$

The above equations are coded in Matlab and below are given an excerpt of the T2 and T3 block elements code. The code for the rest of the block elements is similar.

```
U2 = 0.9765*U1 +0.074;
plot(U1,U2);
grid on
title('T2');
xlabel('y text [A]', 'fontsize',12);
ylabel('z text','fontsize',12);
```

```
  %legend('simulation','data');
  set(legend('EKV                    lc
simulation','BSIM3v3
data',2),'fontsize',12);
  pause;
  I2 = -0.00011*U2.^3 + 0.00032*U2.^2
+ 0.0012*U2 + 0.0081;
  load('fig3_1btl_t181og1.dat');
  U2exp = fig3_1btl_t181og1(:,1);
  I2exp = fig3_1btl_t181og1(:,2);
  plot(U2,I2,U2exp,I2exp,'ro');
  grid on
  title('T2');
  xlabel('U2 [V]', 'fontsize',12);
  ylabel('I2','fontsize',12);
  % legend('simulation','data');
  set(legend('simulation','data',1),'f
ontsize',12);
  pause;


  U3 = 1.0321*U2 +0.0519;
  plot(U2,U3,'linewidth',2);
  set(gca,'fontweight','b','fontsize',
14)
  grid on
  title('T3');
  xlabel('U2 [V]');
  ylabel('U3 [V]');
  %legend('simulation','data');
  set(legend('simulation','data',1),'f
ontsize',12);
  pause;
  I3 = 0.00013*U3.^3 -0.0003*U3.^2 -
0.0018*U3 +0.0104;
  load('fig3_1btl_t160og1.dat');
  U3exp = fig3_1btl_t160og1(:,1);
  I3exp = fig3_1btl_t160og1(:,2);

  plot(U3,I3,U3exp,I3exp,'ro','linewid
th',2);
  set(gca,'fontweight','b','fontsize',
14)
  grid on
  title('T3');
  xlabel('U3 [V]');
  ylabel('I3 [pA]');
  % legend('simulation','data');
  set(legend('simulation','data',1),'f
ontsize',12);
  pause;
```

Some of the block-element equations in Verilog A are given below. The rest of the equations are similar.

```
  Verilog A code:
  //  VerilogA  for  Verilog,  M182N,
veriloga
  `include "constants.h"
  `include "discipline.h"
  module M182N (x, y, g);
  inout x, y, g;
  electrical x, y, g;
  electrical Vin;
   analog
     begin

     V(Vin) <+ V(x, g);
     V(y) <+ V(Vin);
     I(x, y) <+ 8*10e-5* V(y)* V(y)*
V(y)* V(y)- 7*10e- 5*V(y)* V(y)* V(y)-
0.001* V(y)* V(y)+ 0.0048* V(y)+
0.2516;
     end
      endmodule


  //  VerilogA  for  Verilog,  T160OG1,
veriloga
  `include "constants.h"
  `include "discipline.h"
  module T160OG1 (x, y, g);
  inout x, y, g;
  electrical x, y, g;
  electrical Vin;
   analog
     begin

     V(Vin) <+ V(x, g);
     V(y) <+ 1.0321*V(Vin)+0.0519;
     I(x, y) <+ 0.00013* V(y)* V(y)*
V(y) - 0.0003* V(y)* V(y)- 0.0018*
V(y)+ 0.0104;
       end
  endmodule
```

3 Simulation results

3.1 DC analysis

DC analysis is performed at input voltage between –2 and + 3 V. We analyze the change of output voltages and currents, i.e. the output voltages versus the input voltage characteristic and the output currents versus the output voltages characteristic.

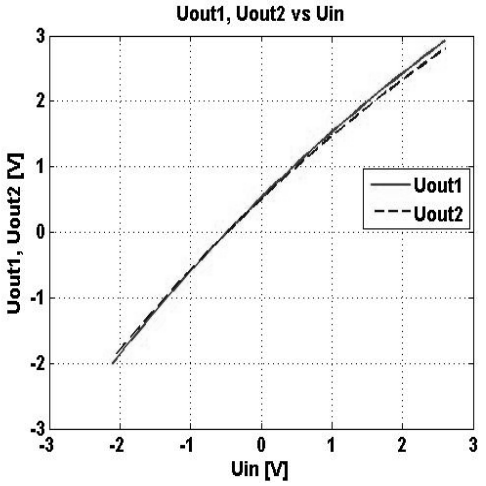

a)

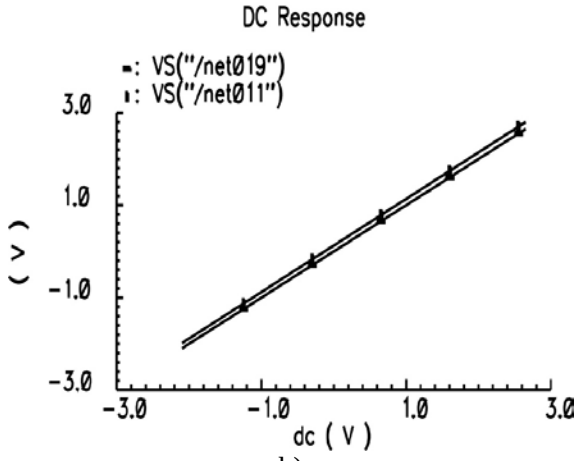

b)

Fig.6. Outputs voltages vs. input voltage a) in Matlab b) in Cadence.

The output voltages are shown in Fig. 6. They are linearly dependent on the input voltage.

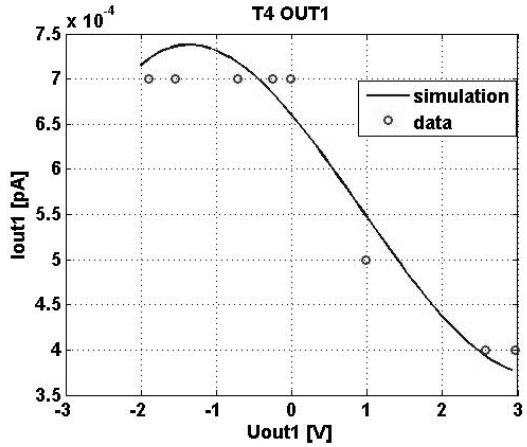

a)

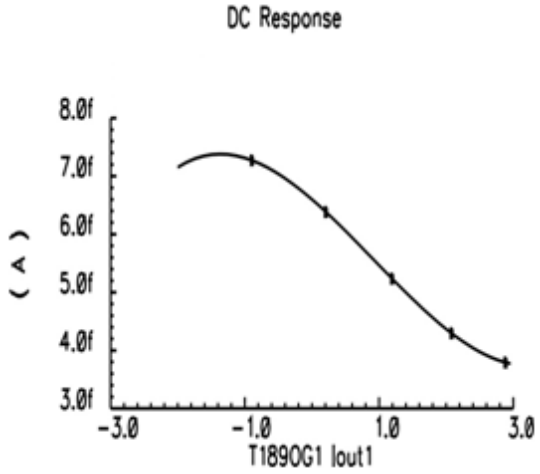

b)

Fig.7. I-V characteristic of output 1 a) in Matlab b) in Cadence..

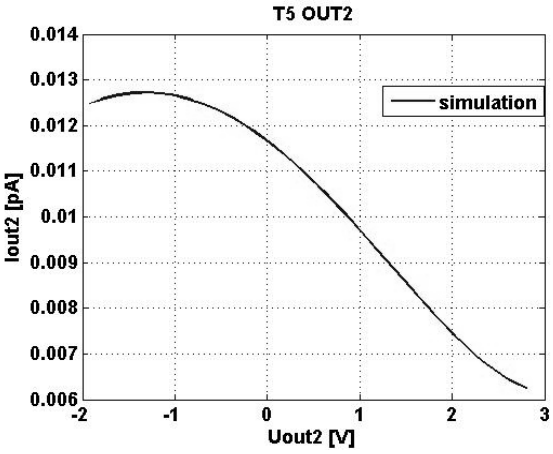

a)

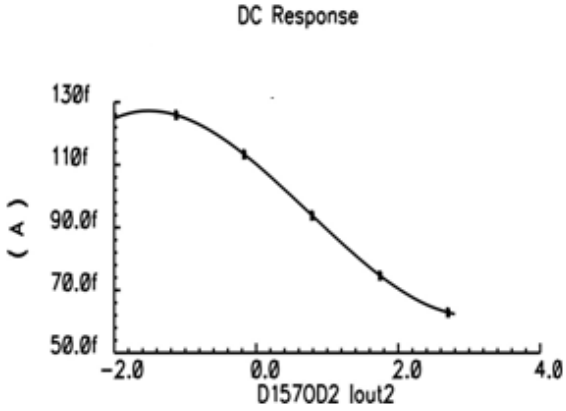

b)

Fig.8. I-V characteristic of output 2 a) in Matlab b) in Cadence..

The *I-V* characteristics of both outputs (Fig. 7 and Fig. 8) can be split in two parts. For voltages between –2 to – 1 V the output currents do not change significantly (first operation region). Hence, the circuit can operate as a current mirror with

different currents in its outputs. At output voltages over –1 V (second operating region) the circuit behaves like an amplifier.

In the second operating region (between –1 and 3 V) the circuit can be regarded as a digital switch.

3.2 Transient analysis

The transient analyses is performed by feeding sine-shaped input voltage with amplitude of +2 [V] and frequency of 10 [GHz]. The results are given in Fig. 9 – 13. The maximum working frequency of the hydrogen bonding network is around 100 [GHz] shown also in Matlab simulations.

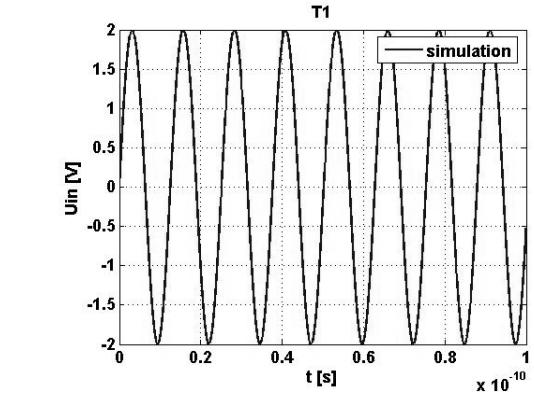

a)

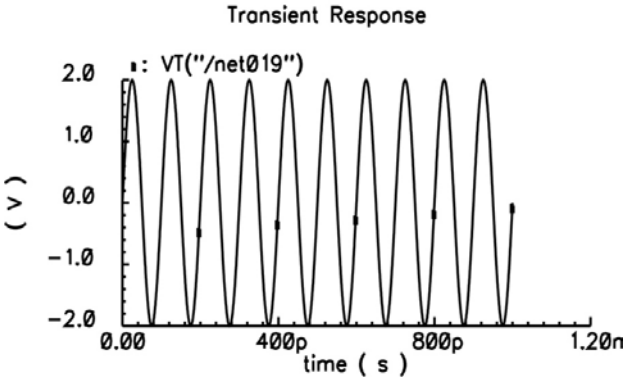

b)

Fig.9. Input voltage vs. time a) in Matlab b) in Cadence.

The input voltage in both simulations (Fig. 9a, 9b) have sine wave form and equal amplitude. The voltages at output 1 and output 2 are with similar characteristics to the input voltage.

The voltage in the output 1 is shown in Fig. 10, and repeats the shape of the input voltage. The output voltage at the second output is shown in Fig. 11 and it is also repeated in the input shape. The results are identical for the simulations in Matlab and Cadence.

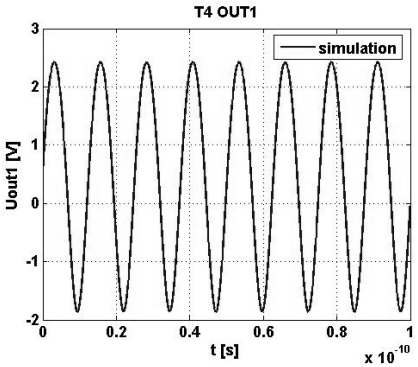

a)

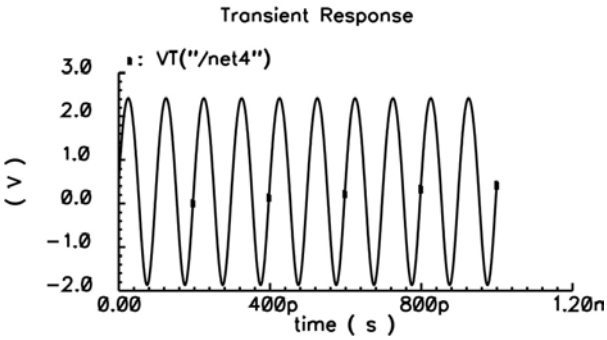

b)

Fig.10. Output voltage at first output vs. time a) in Matlab b) in Cadence..

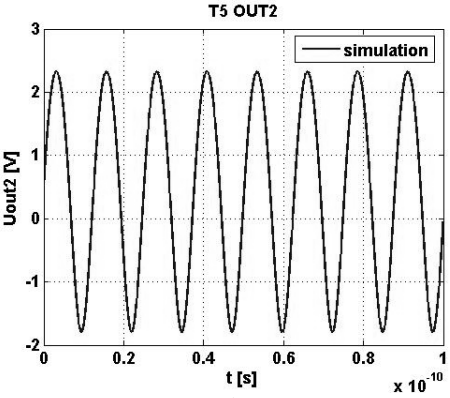

a)

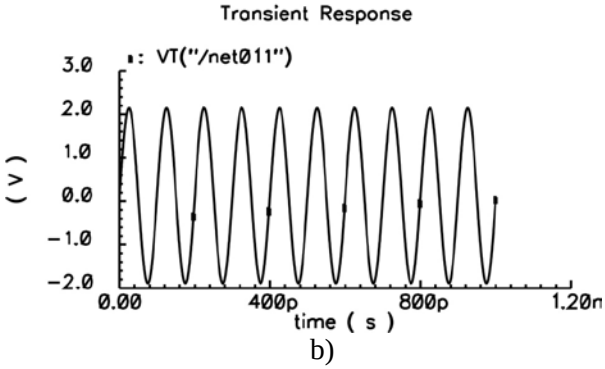

b)

Fig.11. Output voltage at second output vs. time a) in Matlab b) in Cadence..

In both simulations Iout1 is has similar form (Fig. 12a, 12b). There are no differences in frequency and amplitudes. The situation with Iout2 is similar to case of Iout1 – both simulations have similar form, frequency, and amplitude (Fig. 13a, 13b). The circuit realized in Cadence behaves like the circuit modeled in Matlab.

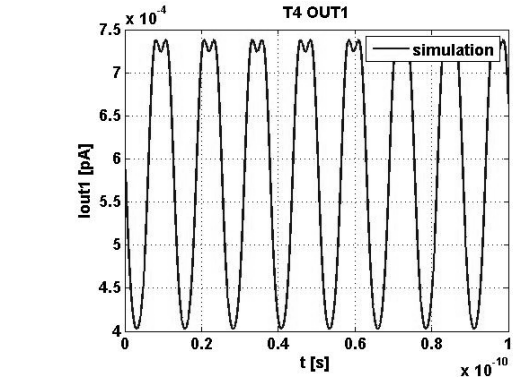

a)

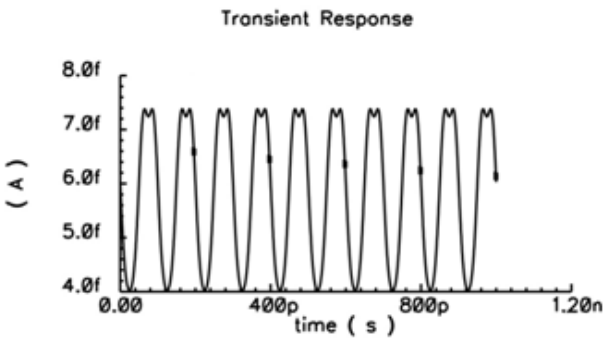

b)

Fig.12. Output current at first output vs. time a) in Matlab b) in Cadence..

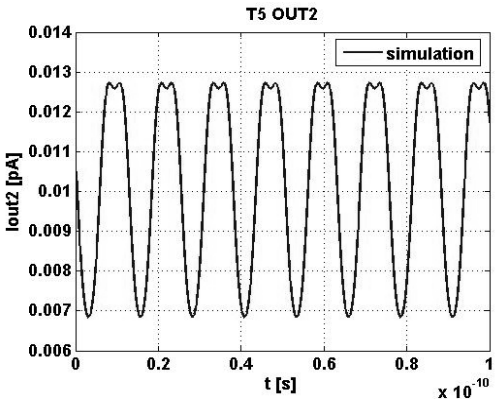

a)

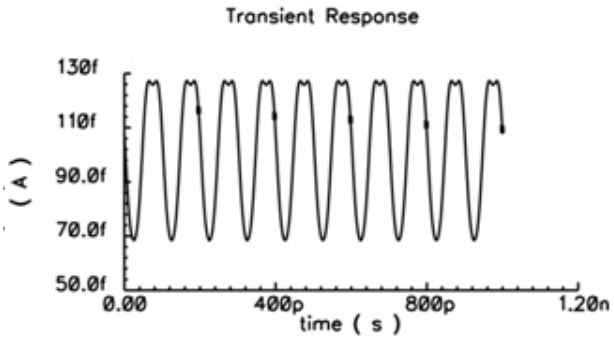

b)

Fig.13. Output current at second output vs. time a) in Matlab b) in Cadence..

Reagrdelss of whether the voltage is postivie or negative the current is always positive.

3.3 Operating levels of the circuit for digital simulation

In order to determine the operating levels and the levels for the input and output logic state “0” and logic state “1” we simulate the transfer characteristic as a function of the output and input currents. The transfer characteristic is given in Fig. 14.

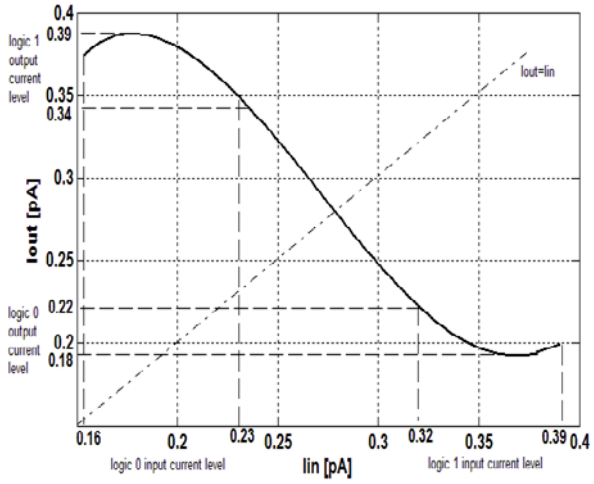

Fig.14. Transfer characteristic of the circuit. The output current as function of the input current.

From the above characteristic, we observe that there are two stable states. We determine the levels for the input and output logic state “0” and logic state “1”.

For the input logic state “0” the levels are between 0.6 to 0.23 pA, for the input logic state “1” the levels are between 0.32 to 0.39 pA.

For the input logic "0" the levels are between 0.18 to 0.22 pA. For the output logic "1" 0.34 to 0.39 pA.

The bias point is at Iout = Iin (the dashed line is at 45°) and the switching is at 0.28 pA.

From the transfer characteristic and the determined logic levels it can be seen that the logic is positive and the logic levels follow the input logic levels which is an essential requirement for digital circuitry.

The tested circuit well represents the properties of the hydrogen bonding network. The developed behavioral model and the preformed DC and transient analyses showed that the network can operate as current mirror, amplifier or decoder. Hence, it can be concluded that based on the proteins and their hydrogen bonding networks new devices and algorithms for information processing can developed.

3.4 Pulse Analysis

The analysis is performed by clock input signal. The input voltage is with different values in order to test how the circuit behaves and to find the logic levels of the input and output following the above determined DC levels for the logic "0" and logic "1".

3.4.1 Input voltage between –2 to +2 V

The input voltage with amplitude 2 V between –2 to +2 V is shown in Fig. 15.

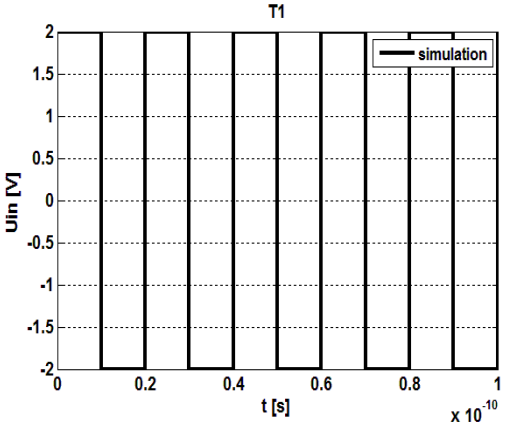

Fig.15. Input voltage versus time.

Input current at input voltage between –2 to +2 V (Fig. 16).

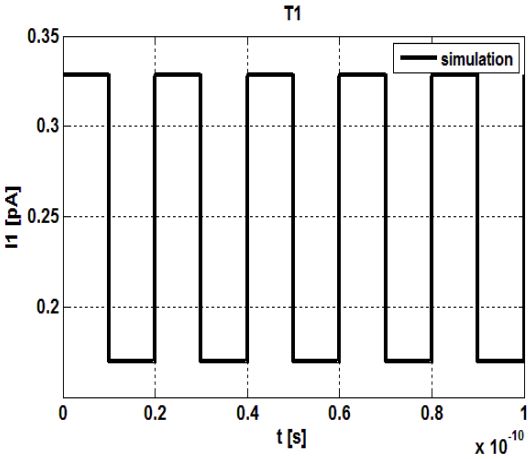

Fig.16. Input current versus time.

Output current at input voltage between –2 to +2 V (Fig. 17).

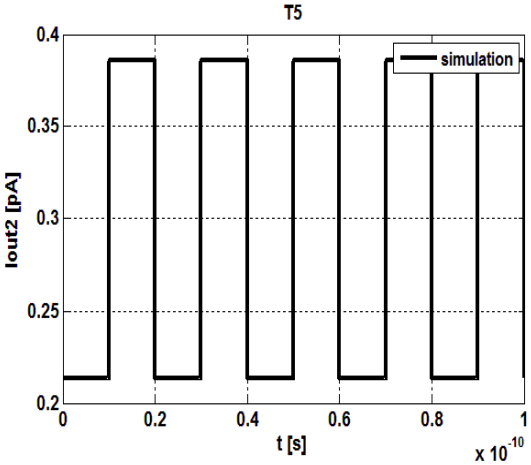

Fig.17. Output current versus time.

It can be seen that the logic levels for logic state "0" and logic state "1" are in the acceptable limits. For the input logic "0" the current 0.16 pA and for the input logic "1" the current 0.33 pA. For output logic "0" the signal is 0.22 pA and for output logic "1" the level is 0.38 pA.

Fig. 8 and 9 show that when logic "1" is fed to the input at the output we obtain logic "0" and vice versa. Hence, the circuit operates as an inverter.

3.4.2 Input voltage between –2 to -1 V

The input voltage with amplitude 1 V between –2 to –1 V is shown in Fig. 18.

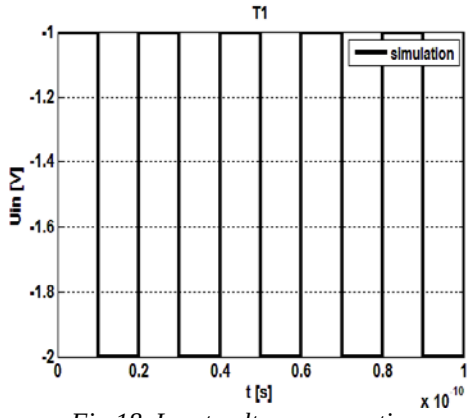

Fig.18. Input voltage versus time.

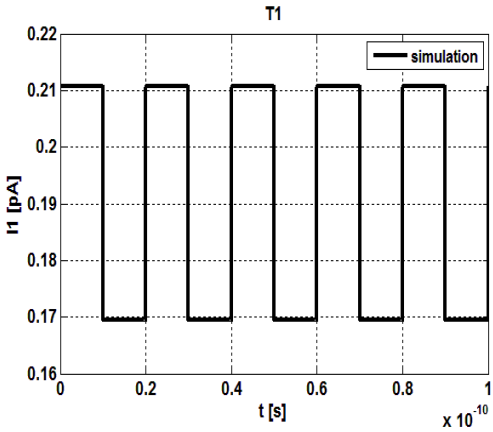

Fig.19. Input current versus time at input voltage between -2 to -1 V.

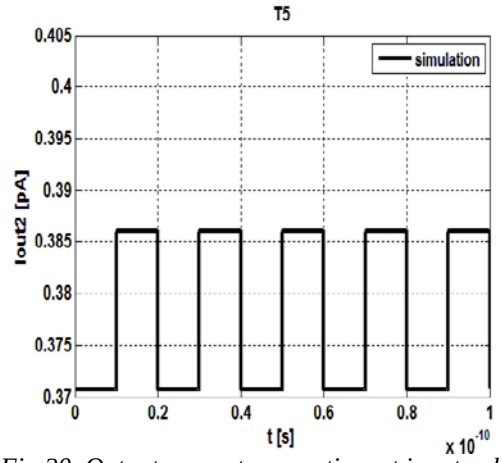

Fig.20. Output current versus time at input voltage between -2 to -1 V.

From the figures above (figures 19 - 20) it can be seen that in the range of the input voltage between –2 to –1 V, the logic levels at the input are all the time in the same intervals as the logic levels for the input “0”; the logic levels of the output signal are all the time in the intervals of the logic levels for output “1”. Hence, in this range of the input voltage the circuit does not operate as any known element.

3.4.3 Input voltage between 2 to 3 V

The input voltage with amplitude 1 V between 2 to 3 V is shown in Fig. 21.

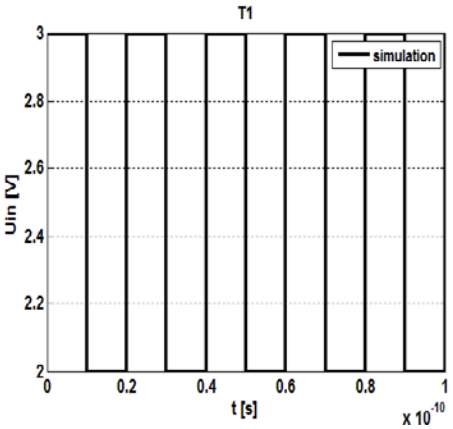

Fig.21. Input voltage versus time.

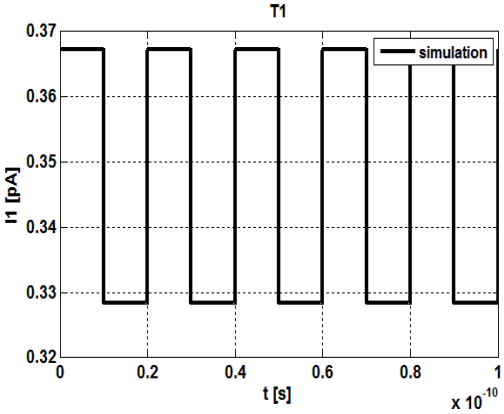

Fig.22. Input current versus time at input voltage between 2 to 3 V.

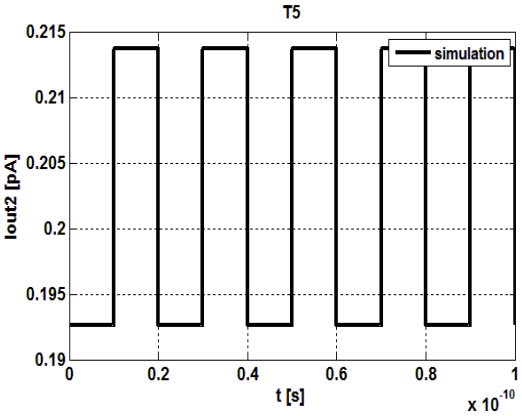

Fig.23. Output current versus time at input voltage between 2 to 3 V.

From the above figures (fig. 22 and 23) it can be seen that in this range of the input voltage (between 2 to 3 V) despite that the input is a clock signal, the amplitude of this clock signal remains all the time in the interval where the input signal is in logic “1” state. The same applies for the output signal: despite

that the output signal is a clock signal, its amplitude remains all the time in the interval where the output signal is in logic "0" state. In this range of the input voltage the circuit does not operate as any known element as well.

The performed analyses prove that the circuit operates well in the input voltage range between –2 and +2 V. In this range it operates as an inverter. When the input voltage is outside this range the logic levels fall in the determined intervals for "0" or "1" and it is not possible to change the input or output – they remain in a stable state (either logic "0" or "1.

4 Conclusion

The studied circuit well describes the operation of the hydrogen bonding network. The developed behavioral model and the performed DC and digital pulse analysis showed that the network behaves similarly to current mirror and amplifier and it can be used also as inverter.

This implies that the same hydrogen bonding networks can operate not only as analog devices but also similarly to digital devices.

Finally, we once again proved that hydrogen bonds might serve as basis for development of new devices and algorithms for signal processing.

6 Acknowledgment

The research in this paper was carried out within the framework of Contract No. DUNK 01/03 dated 12.2009.

References:

[1] Elitsa Gieva, Rostislav Rusev, George Angelov, Rossen Radonov, Marin Hristov and Tihomir Takov, *Protein application in electronics*, 14th International workshop on Nanoscience and Nanotechnology, NANO'2012, 22.11.2012 - 23.11.2012

[2] Claudio Nicolini, *Molecular Bioelectronics*, Singapore NewJersey*London Hong Kong, ISBN 981-02-2685-3, 1996

[3] Evgeniy V. Gromov, Irene Burghardtc, Horst Köppel, Lorenz S. Cederbaum, *"Native hydrogen bonding network of the photoactive yellow protein (PYP) chromophore: Impact on the electronic structure and photoinduced isomerization"*, Journal of Photochemistry and Photobiology A: Chemistry 234 (2012) 123–134

[4] M. Salomé Sirerol-Piquera, Arantxa Cebrián-Silla, Clara Alfaro-Cervelló, Ulises Gomez-Pinedo, Mario Soriano-Navarro, José-Manuel García Verdugo, *"GFP immunogold staining, from light to electron microscopy, in mammalian cells"*, journal Micron 43 (2012) 589–599.

[5] G.E. Adamov, A.G. Devyatkov, L.N. Gnatyuk, I.S. Goldobin, E.P. Grebennikov, "*Bacteriorhodopsin—Perspective biomaterial for molecular nanophotonics"*, Journal of Photochemistry and Photobiology A: Chemistry 196 (2008) 254–261.

[6] Jeffrey A Stuarta, Duane L Marcya, Kevin J Wiseb, Robert R Birgeb, *"Volumetric optical memory based on bacteriorhodopsin"*, Synthetic Metals, Volume 127, Issues 1–3, 26 March 2002, Pages 3–15;

[7] K. L. Kompa and R. D. Levine, *A molecular logic gate*, 410–414, PNAS, vol. 98, no. 2 January 16, 2001

[8] R. Rusev, G. Angelov, T. Takov, M. Hristov *Analogy Between Hydrogen Bonding Network and Microelectronic Circuit*, MIXDES 2009, Proceedings of 16th international conference "Mixed Design of Integrated Circuits and Systems", June 25-27, 2009, Lódz, Poland, pp. 402-405, ISBN 978-83-928756-0-4.

[9] Rostislav Rusev, Boris Atanasov, Tihomir Takov, Marin Hristov, *Microelectronics Models of Protein Hydrogen Bonds*, E+E, pp. 3 – 6, 2009, ISSN 0861-4717

[10] Markus A., V. Helms (2001). *Compact Parameter Set for Fast Estimation of Proton Transfer Rates*, J. Phys. Chem., 114(3), http://dx.doi.org/10.1063/1.1332993.

[11] D. Fitzpatrick, I. Miller, *Analog Behavioral Modeling with the Verilog-A Language*, Kluwer Academic Publishers, New York, Boston, Dordrecht, London, Moscow, 2003, pp 41-86, ISBN: 0-7923-8044-4

[12] http://www.cadence.com/ Products, Custom IC Design (2013).

[13] David N. Silverman, *"Marcus rate theory applied to enzymatic proton transfer"*, Biochimica et Biophysica Acta (BBA) – Bioenergetics, Volume 1458, Issue 1, 12 May 2000, Pages 88–103

[14] Matlab site http://www.mathworks.com/